Laboratory-scale evaluation of secondary alkaline zinc batteries for electric vehicles

Kathryn A. Striebel, Frank R. McLarnon and Elton J. Cairns
Energy and Environment Division, Lawrence Berkeley Laboratory and Department of Chemical Engineering, University of California, Berkeley, CA 94720 (USA)

(Received and accepted March 8, 1993)

Abstract

Two types of secondary zinc cell have been evaluated in our laboratory to assess their suitability to power an electric van. Single cells were charged and discharged with constant-current cycles as well as with controlled-power discharge profiles, scaled to the predicted mass of a full-size battery. Both cells were able to meet the requirements for power discharge specified by the so-called Simplified Federal Urban Driving Schedule (SFUDS) early in life (the first 15 cycles). The Zn/air cell achieved an average of 72 SFUDS repetions (7.2 h) per discharge. The Zn/NiOOH cell achieved an average of 51 SFUDS repetitions (5.1 h) per discharge. The bifunctional air electrodes did not reach oxygen-evolution potentials during the 8-s regenerative breaking portions of the SFUDS cycle.

Introduction

Secondary alkaline zinc batteries have been studied for many years and were the subject of a recent review [1]. Sealed and vented cells with pasted Zn negative electrodes and sintered nickel oxide positive electrodes have exhibited 55–85 Wh/kg specific energy (in comparison with a theoretical value of 326 Wh/kg) with very high specific power (170–260 W/kg) [2–5]. The shape change of the Zn electrode during cycling, a major life-limiting factor, has been found to be controllable with novel electrolyte compositions which lower the solubility of the migrating zincate species in the battery, and sealed cells show the additional promise of eliminating zinc dendrite formation by oxidation [6].

The Zn/air cell has an even higher theoretical specific energy (1300 Wh/kg, assuming an oxygen cathode) primarily due to the unlimited supply of air for the positive electrode. Another technique for overcoming shape change in the Zn electrode is to use a reticulated-zinc flow-through electrode, invented by Ross [7]. Forced convection of the 45 wt.% KOH electrolyte carries dissolved Zn to the foam substrate during charge and away from it during discharge. Putt [8] has demonstrated over 800 cycles with this electrode in a Zn/Zn cell. The development of a long-lived bifunctional air electrode is proceeding in our laboratory and elsewhere. Published work with these types of cells consists primarily of steady-state, constant-current, constant-potential or constant-power profiles during charge and/or discharge. Of foremost concern, however, is whether or not these cells can provide the necessary transient power response required for vehicle applications. We have tested laboratory-size cells with the Simplified Federal Urban Driving Schedule (SFUDS) power-time profile. Emphasis has been

0378-7753/94/$07.00

placed on comparison of the steady-state and transient responses of the individual electrodes in these cells in an effort to identify potential problems encountered with such power profiles that cannot be anticipated from steady-state results.

Battery calculations

The SFUDS power profile specifies power requirements for typical urban vehicle driving, scaled to the mass of the battery power source. When comparing the performance of laboratory cells, a method of scaling the mass of the battery needs to be devised because auxiliary equipment (cell case, pumps, etc.) will always constitute a higher fraction of total system mass for a smaller active area of the battery/cell system. Design calculations for batteries which fulfill the volume, energy and power requirements for the so-called Improved Dual-Shaft Electric Propulsion (IDSEP) van [9] are summarized in Table 1. The electrode and separator mass for the Zn/NiOOH cell are scaled from laboratory-cell data, combined with estimated mass for the cell case and hardware. The Zn/air cell figures were taken directly from values reported in a paper design by Putt [10]. Both designs are based on monopolar cells because suitable bipolar plate materials are not available for these types of cells. The loading for the Zn/air cell is 35 mAh/cm^2 interfacial area. The Zn/NiOOH cell has a design loading of 15.7 mAh/cm^2 interfacial area. The actual loading of ZnO is three times this amount to improve cycling characteristics and life. These calculations lead to scaling factors of 4.2 and 5 kg battery per m^2 of anode/cathode interfacial area, for the Zn/NiOOH and Zn/air batteries, respectively. These factors allow comparison of the SFUDS performance of the two cells on an equivalent battery mass basis. This type of comparison gives the Zn/air cell some advantages. First, the predictions for the Zn/air battery may be optimistic, whereas those for the Zn/NiOOH battery are based on laboratory data for actual cell components. Second, the mass of Zn/air battery that will fit on-board an IDSEP van will be limited by the maximum volume limit because of its relatively low capacity density of 71 Ah/l. The Zn/NiOOH battery has a capacity density of around 120 Ah/l allowing more mass of Zn/NiOOH battery on the van.

TABLE 1

Battery calculations

Zn/NiOOH – 22400 Ah			Zn/Air – 36000 Ah		
Component	g/Ah	kg total	Component	g/Ah	kg total
NiOOH electrode	8.4	188	Air electrode	0.6	20
Zn electrode	6.7	150	Zn electrode	1.9	68
Electrolyte	9.0	202	Electrolyte	7.9	284
Separator and wick	1.2	27	Separator and wick	0.2	8
Cell case and hardware	1.5	34	Cell case and hardware	3.2	117
Total mass	26.8	600	Total mass	13.8	497
Zn loading (Ah/m^2)		157	Zn loading (Ah/m^2)		360
Interfacial area (m^2)		143	Interfacial area (m^2)		100
Scale factor (kg/m^2)		4.2	Scale factor (kg/m^2)		5
Average cell voltage (V)		1.6	Average cell voltage (V)		1.2
Specific energy (Wh/kg)		60	Specific energy (Wh/kg)		87

Laboratory cells

The Zn/NiOOH cells tested in our laboratory have been described in detail in refs. 2 and 6. The nominal 1.35 Ah cells were constructed from a single pasted zinc electrode surrounded by two sintered NiOOH positive electrodes. As mentioned above, the Zn electrode contained 4.17 Ah ZnO (3 times the rated capacity) and was prepared from two slurry cakes pressed onto 6 cm×7 cm Pb-plated Cu mesh current collectors. This electrode is enveloped in three layers of Celgard 3401 (Hoechst–Celanese Corp., Charlotte, NC) microporous polypropylene separator. The positive electrodes were purchased from Eagle–Picher Industries, Inc. and had a rated capacity of 15.5 mAh/cm^2. They were encased in a single layer of Pellon 2524 (Freudenberg Nonwovens, Chelmsford, MA) wicking material. The cell was vacuum-filled with 17 wt.% KOH electrolyte containing about 27 wt.% supporting electrolyte (2 M K_2CO_3 and 2 M KF) and presaturated with ZnO. This electrolyte was chosen to improve ionic conductivity and reduce shape change in the Zn electrode [6]. An Hg/HgO reference electrode was connected to the cell case with a capillary leading to the side of one of the wick-surrounded positive electrodes. With this arrangement, the cell IR loss is contained within the negative electrode potential measurement.

The Zn/air cell was constructed from a single flow-through Zn electrode and two bifunctional air positive electrodes. The negative electrode substrate was a 6.4 mm thick 5 cm×5 cm reticulated copper foam substrate, obtained from Foametal Inc., Willoughby, OH. This foam has a porosity of 97% and was plated with a 0.7 Ah coat of dense Zn to protect the Cu substrate from corrosion. Developmental bifunctional air electrodes (AE100 BF8-2) were obtained by courtesy of Electromedia Corp., Englewood, NJ). These electrodes were constructed with Ni screen current collectors on both sides and are catalyzed with cobalt tetramethoxyphenylporphyrin (CoTMPP) to catalyze the oxygen reduction and a Ni–Co spinel to catalyze oxygen evolution. They are reported to withstand more than 100 cycles in 30 wt.% KOH electrolyte in the absence of zincate in solution [11]. The cell was assembled with three layers of Celgard 3401 separator on both sides of the Zn electrode and a layer of ZYK-15 zirconia cloth (Zircar Products Inc., Florida, NY) wick next to each air electrode.

The circulating electrolyte contained 45 wt.% KOH with 40 g/l Zn at the beginning of the first charge half-cycle. The reservoir contained between 60–100 ml electrolyte (electrolyte was added periodically to account for small leaks around the air electrode into the air chamber which prevented exact knowledge of the electrolyte composition). The ratio of circulation-system volume to cell area was too large to permit cycling over the complete range of interest for practical battery design. The composition chosen allowed cycling down to the recommended lower limit of zincate concentration (15 g/l Zn). Only small Zn electrode polarizations were observed, consistent with observations by Ross [7], except after prolonged unattended cycling when reservoir volume was depleted due to leakage, and the inventory of Zn was therefore too low. The depletion of zincate was signaled by a rapid rise in the Zn electrode overpotential during charge and subsequent (computer-controlled) cutoff of the charge half-cycle. The electrolyte flow rate was approximately 4 ml/min, which is significantly higher than that required to maintain an essentially uniform composition over the flow direction through the foam at the current densities employed [12].

Air was scrubbed and humidified by passing it through a 1 M KOH bath prior to entering the air electrode compartments. Air-flow rates of more than 10 times the stoichiometric value were used during discharge. The gas-flow rate affected air electrode overpotentials only at the highest current densities, indicating losses due to gas-phase

mass transfer. The air-flow rate was lowered somewhat during cell charging in order to minimize the rate of dryout of the scrubbing bath. A Hg/HgO reference-electrode compartment was filled from the flowing electrolyte through a capillary connection to the Zn electrode frame. With this arrangement, the ohmic potential drop across the cell is included in the air electrode potential reading.

Test hardware

Cell cycling was carried out automatically for each half-cycle. Constant-current performance curves as well as SFUDS profile tests were carried out with an analog bi-directional current controller which was computer-controlled with an IBM PC and a Tecmar data acquisition card. Two digital I/O channels controlled the logic for the current controllers (cell on/off and charge/discharge). One D/A line was used to set the current (0–5 A). The electrode potentials were measured with A/D converters; the reference electrode potential was measured by means of a high-impedance voltage follower. Current was recorded directly with two A/D converters connected across an internal shunt in the current controller. Ohmic potential drop was measured separately with a conductivity bridge connected between the anode and cathode current collectors. In the Zn/NiOOH cell, this value was essentially constant at about 20 mΩ. However, in the Zn/air cell this resistance varied considerably from about 100 to 400 mΩ between end-of-charge (EOC) and end-of-discharge (EOD), respectively, as will be discussed later. In some cycles this resistance rose as high as 650 mΩ, leading to a failure of the cell to meet the peak power requirement.

Constant current cycling results

Charging was carried out at the *C*/6 rate (2.6 mA/cm^2) for the Zn/NiOOH cell to allow comparison with previous results. Taper charging, often used with this type of cell to reduce gassing by the positive electrode [2], was not used in this work. Discharge capacities for the first five cycles were used to determine the '100%' capacity of the cell as 1.27 Ah, which was limited by the Ni electrodes. This is equivalent to 98% of the theoretical value based on the mass of the active material and is consistent with previous results in the lower alkalinity electrolytes. For cycles 6–15, charge capacity was limited to 1.32 Ah (4% overcharge to account for the inefficiency of the Ni electrode) or a cell cutoff voltage of 2.0 V, whichever was reached first.

Charging of the 1.8 Ah Zn/air cell was carried out at constant current at the *C*/12 rate (3 mA/cm^2) to a charge cutoff limit of 2.0 Ah (10% overcharge). The large amount of overcharge was used to ensure that excess capacity was always available to avoid discharging into the dense Zn-protective layer, until enough operating experience was gained with this cell. This layer should discharge at potentials of about 5 mV cathodic to the mossy Zn deposited during charge [13], however, this 5 mV change was difficult to detect with our control system, especially when discharging with the SFUDS power profile.

Potential and current data for charge and discharge half-cycles of these two cells are compared in Figs. 1 and 2. All Zn electrode potentials are shown as reference versus Zn potential to provide better plotting resolution. The Zn/air cell voltage remains essentially constant during charge at an average of 2.01 V ($E_{Zn} = -1.381$ and $E_{air} = 0.627$) except when the zincate was depleted from the electrolyte (not shown), as mentioned

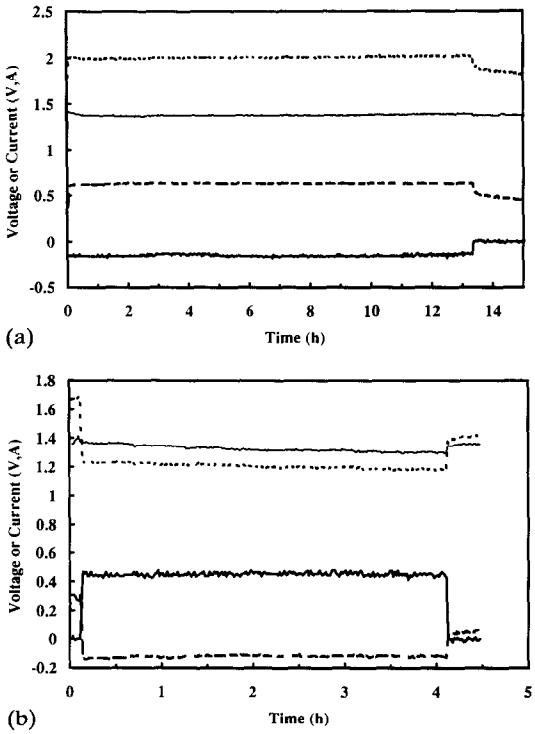

Fig. 1. Constant-current cycle data for 1.8 Ah Zn/air cell, cycle 9: (a) *C*/12 charge, and (b) *C*/4 discharge; (——) $-E_{Zn}$, (----) E_{cell}, (– – –) E_{air}, and (——) current.

earlier. The Zn/NiOOH cell potential changes with state-of-charge with an average cell potential of 1.808 V ($E_{Zn} = -1.387$ and $E_{Ni} = 0.421$). Some of this variation is due to polarization of the Zn electrode, however the behavior is dominated by change in E^0 of the nickel oxide electrode with state-of-charge. Both cells were discharged at a constant current *C*/4 rate corresponding to 3.8 and 9 mA/cm^2 for the Zn/NiOOH and Zn/air cells, respectively. Again, the Zn/air cell discharge voltage remains essentially constant at an average value of 1.206 V ($E_{Zn} = -1.326$ and $E_{air} = -0.120$). The shape of the discharge curve for the Zn/NiOOH cell is again dominated by the nickel oxide electrode with an average cell potential of 1.555 V ($E_{Zn} = -1.277$ and $E_{Ni} = 0.279$).

Steady-state polarization

Steady-state polarization measurements were recorded by setting a constant current and recording potential values at 5-s intervals until three successive measurements were constant, which usually required about 30 s. These measurements were carried out during several discharge half-cycles for the Zn/air cell because of apparent degradation of the cell performance. Measured cell resistances were recorded in order to correct the air electrode potentials and identify the source of the performance loss. Measured air electrode potentials are shown in Fig. 3, along with IR-corrected values for cycles 2, 8, 14 and 15. These results indicate that the decrease in performance was primarily due to increases in cell resistance. Cell resistance was always lower at the EOC than

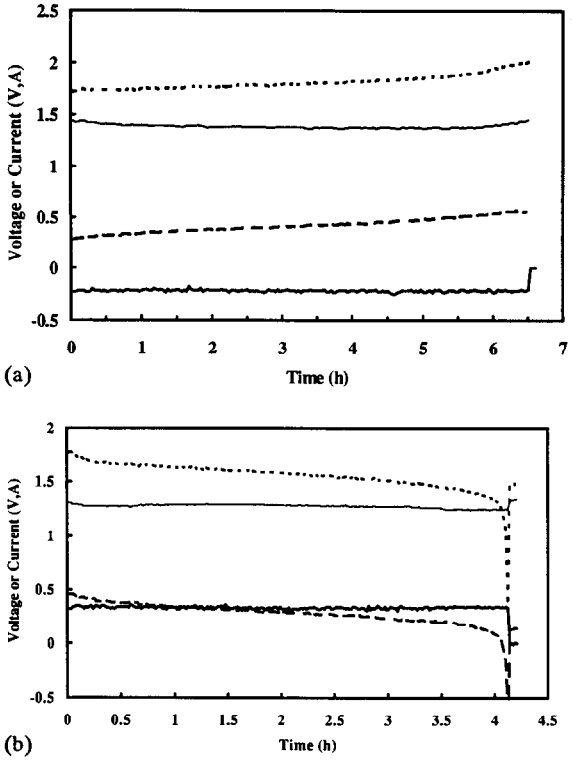

Fig. 2. Constant-current cycle data for 1.3 Ah Zn/NiOOH cell, cycle 12: (a) *C*/6 charge, and (b) *C*/4 discharge; (——) $-E_{Zn}$, (----) E_{cell}, (– – –) E_{NiOOH}, and (——) current.

at the EOD, suggesting that Zn was depositing in the interelectrode gap instead of inside the foam. This phenomenon was probably caused by incomplete compression of the separator and/or irreversible compression of the Foametal substrate. The SFUDS peak power required for the Zn/air cell was 2 W, which was available until cycle 13. SFUDS results from cycle 6 are included for comparison in Fig. 3. These will be discussed later.

Steady-state polarization measurements were made at the beginning, middle and EOC during discharge #6 of the Zn/NiOOH cell. These data are shown in Fig. 4, together with the calculated power. The peak SFUDS power required for this cell is 2.77 W, which can be met at all states-of-charge and did not deteriorate over 15 cycles.

SFUDS discharges

The SFUDS power profile was scaled to the estimated battery mass, as discussed above, to yield two different profiles for discharging the two Zn cells. The 6-min profiles contain 20 segments at 6 different power levels (0, +10, +20, +50, +79 and −10 W/kg). They are repeated continuously until EOD is reached, as determined by either a capacity limit or a mininum cell voltage. Because the Zn/air cell and electrode potentials were essentially invariant with the state-of-charge, a capacity limit of 1.8 Ah was used as EOD criterion. In the Zn/NiOOH cell, EOD was defined as

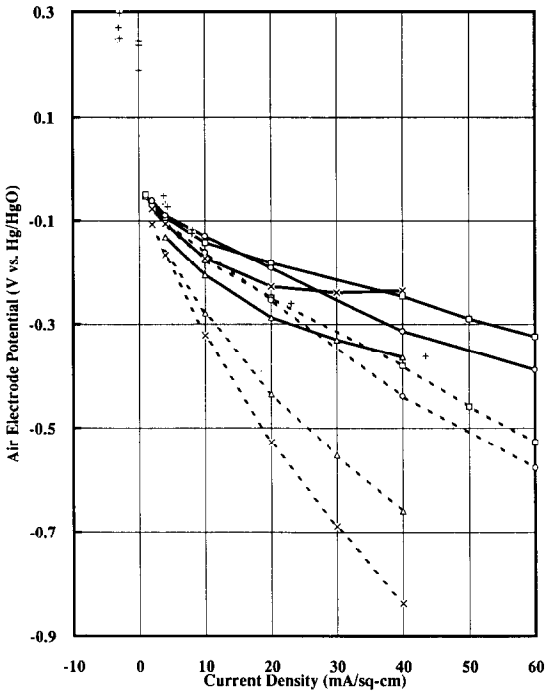

Fig. 3. Air electrode polarization curves for 1.8 Ah Zn/air cell for different cycles: (□) cycle 2, (○) cycle 8, (△) cycle 14 and (×) cycle 15; (——) IR-corrected, (----) raw data, and (+) SFUDS discharge data from cycle 6.

the time when cell voltage dropped below 1.0 V (which always occurred during the highest power segment (≠15)). Power profiles, currents and individual electrode potentials recorded during SFUDS discharges with cells during the middle of discharges 6 and 8 for Zn/air and Zn/NiOOH, respectively, are shown in Fig. 5. The power curves indicate that both cells can adequately supply the necessary power for SFUDS, at least very early in life. The profiles for the Zn/air cell are characterized by extremely flat Zn electrode potentials and widely varying air electrode potentials. The air electrode data are replotted with the steady-state polarization data in Fig. 3. These values are close at an all power levels except during the regenerative breaking (charging) segments of the SFUDS profile. The relatively low air electrode potentials exhibited during regenerative braking indicate that the charging currents are not due to oxygen evolution (compare with charging potentials in Fig. 1(a)). This phenomenon could possibly be caused by oxidation of the peroxide ion generated during the discharge (an intermediate product in the oxygen/reduction reaction), however CoTMPP is considered to be an excellent peroxide-decomposition catalyst [14]. Alternatively, pseudo- or double-layer capacitive processes are most likely responsible for this process. The Co and/or Ni sites in the charge catalyst can undergo redox processes in this potential range [15]. The exact loading of the $NiCo_2O_4$ was not available however, so quantification of this process is not possible.

Summary plots of these SFUDS discharges are shown in Fig. 6 as average potential during five different segments, (2, 3, 4, 15 and 16) corresponding to the five non-zero power levels (10, 20, −10, 79 and 50 W/kg) as a function of repetition number.

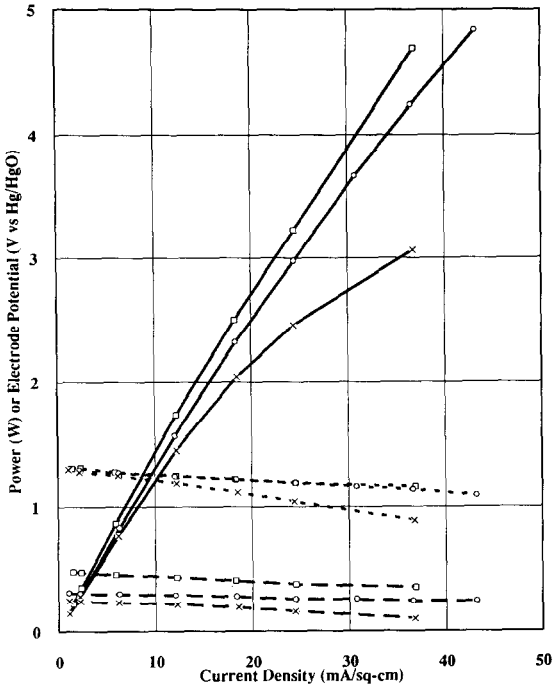

Fig. 4. Power and electrode polarization curves at three states-of-charge for 1.3 Ah Zn/NiOOH cell: (□) beginning of discharge, (○) middle of discharge, (×) end-of-discharge; (——) power, (----) $-E_{Zn}$, and (– – –) E_{NiOOH}.

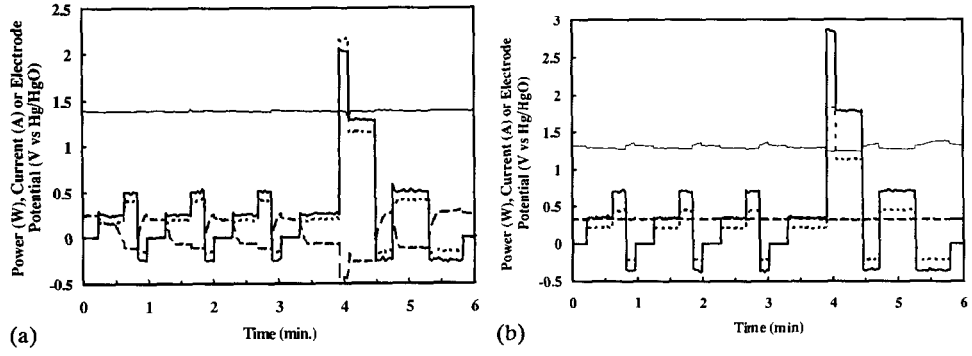

Fig. 5. SFDUS repetition (a) during cycle 6 discharge for 1.8 Ah Zn/air cell, and (b) during cycle 7 discharge for 1.3 Ah Zn/NiOOH cell: (——) power, (——) $-E_{Zn}$, (– – –) E_{air} or E_{NiOOH}, and (----) current.

Comparisons of these curves indicate that the Zn electrode in the forced-convection cell is significantly less polarizible with increasing state-of-discharge than the pasted Zn electrode in the static electrolyte cell. However, the polarization behaviors of the respective positive electrodes are reversed. The mass and relative complexities of these

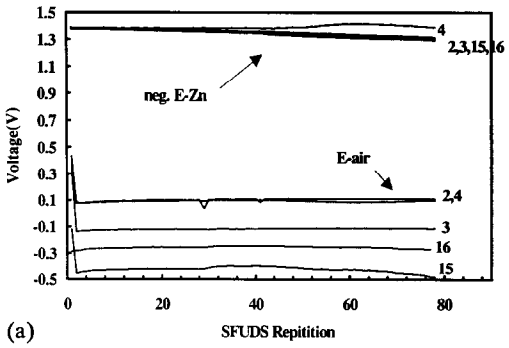

(a)

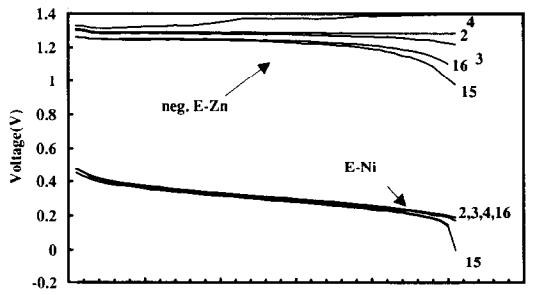

(b)

Fig. 6. Average potentials during segments 2, 3, 4, and 15 of SFDUS discharges for (a) cycle 6 of the 1.8 Ah Zn/air cell, and (b) for cycle 7 of the 1.3 Ah Zn/NiOOH cell.

four electrodes would suggest that a pasted-electrode Zn/air cell might be a good electrode combination, but these results indicate that the polarizability would be poorest for such a combination.

Charge and discharge capacities for the first 15 cycles of these cells are listed in Table 2. Generally lower utilization was encountered for the Zn/NiOOH cell during the SFUDS discharges as compared with the constant-current discharge cycles. The 1 V cutoff was always reached during the peak power segment of the SFUDS discharge because of the increase in polarizability at the EOD. The polarizability of the Zn/air cell is greater over the entire discharge but it is so constant that utilization is 100% for this cell regardless of which discharge used. However, one might expect that the variable power levels might lead to premature degradation of the life of the air electrode. This is the subject of future work.

Conclusions

Zinc/air and Zn/NiOOH cells have been cycled with constant-current and controlled-power (SFUDS) discharges for up to 15 cycles. Preliminary results indicate that both types of cell are capable of providing the power required for electric vehicle applications. The short-term charging during the regenerative braking portion of the discharge appears to be carried by pseudo-capacitive currents in the Zn/air cell.

TABLE 2

Charge/discharge history of laboratory alkaline zinc cells

Cycle no.	1.8 Ah Zn/air cell				1.27 Ah Zn/NiOOH cell			
	C/12 charge (Ah)	Type of discharge	Discharge (Ah)	Capacity (%)	*C*/6 charge (Ah)	Type of discharge	Discharge (Ah)	Capacity (%)
1	1.82	*C*/4	1.80	100	1.35	*C*/2.5	1.28	101
2	1.97	SFUDS, perf.	1.59	88	1.34	*C*/2.5	1.27	100
3	1.97	MSFUDS	1.05	58	1.34	*C*/2.5	1.28	101
4	1.61	*C*/4	1.61	90	1.34	*C*/2.5	1.27	100
5	1.78	*C*/4	1.80	100	1.34	*C*/2.5	1.27	100
6	1.97	SFUDS	1.80	100	1.32	*C*/4, perf.	1.28	101
7	1.97	MSFUDS	1.81	101	1.32	SFUDS	1.21	95
8	1.98	*C*/4, perf.	2.17	121	1.33	MSFUDS	1.24	98
9	1.98	*C*/4	1.80	100	1.33	SFUDS	1.20	95
10	1.97	SFUDS	1.80	100	1.32	MSFUDS	1.22	96
11	1.97	SFUDS	1.80	100	1.64	*C*/4	1.39	110
12	1.97	SFUDS, perf.	2.05	114	1.43	*C*/4	1.37	108
13	1.97	SFUDS	1.25	69	1.40	SFUDS	1.20	95
14	1.97	*C*/4	1.80	100	1.23	MSFUDS	1.21	95
15	1.97	*C*/4, perf.	1.00	56	1.21	SFUDS	1.18	93

SFUDS = Simplified Federal Urban Driving Schedule.
MSFUDS = Modified Simplified Federal Urban Driving Schedule, regenerative breaking segment set to 0 power.
perf. = performance curve recoded during the cycle.

Acknowledgements

This work was supported by the Assistant Secretary for Conservation and Renewable Energy, Office of Transportation Technologies, Electric/Hybrid Propulsion Division, of the US Department of Energy under Contract No. DE-AC03-76SF00098.

References

1 F.R. McLarnon and E.J. Cairns, *J. Electrochem. Soc., 138* (1991) 645.
2 J.T. Nichols, F.R. McLarnon and E.J. Cairns, *Chem. Eng. Commun., 37* (1985) 355.
3 T.C. Adler, F.R. McLarnon and E.J. Cairns, *Proc. 22nd Intersoc. Energy Conversion Engineering Conf., 1987,* American Institute of Aeronautics and Astronautics, New York, USA, p. 1097.
4 A. Charkey, *Proc. 10th Intersoc. Energy Conversion Engineering Conf., 1975*, Institute of Electric and Electronic Engineers, New York, USA, p. 1126.
5 E.H. Hietbrink, R.W. Bonk and R.L. Corbin, *Ext. Abstr., Electrochemical Society Meet., 1982*, The Electrochemical Society, Pennington, NJ, USA, Vol. 82-2, Paper No. 16.
6 T.C. Adler, F.R. McLarnon and E.J. Cairns, *J. Electrochem. Soc., 140* (1993) 289.
7 P.N. Ross, Jr., *US Patent No. 4 842 963* (June 27, 1989).
8 R. Putt, *Lawrence Berkeley Laboratory Rep. No. LBL-29 078, Final Rep.,* May 1990.
9 G.H. Cole, Society Automotive Engineers, Tech. Paper Ser. No. 891 664, A generic SFUDS battery test cycle for electric road vehicle batteries, *Future Transportation Technology Conf. Exposition, Vancouver, BC, Canada, Aug. 7, 1989.*
10 R. Putt, *Zinc–air Design Concept for the DOE-EHP IDSEP Van,* Matsi Inc., July 31, 1990.
11 F. Solomon, personal communication.
12 P. Foller, *J. Appl. Electrochem., 16* (1986) 527.
13 L. McVay, personal communication, 1991.
14 D. Tryk, W. Aldred, Z. Chen, C. Fierro, J. Hashiguchi, M. Hossain, Z. Zhang, F. Zhao and E. Yeager, *Lawrence Berkeley Laboratory Rep. No. LBL-19 003, Final Rep.,* Jan. 1985.
15 R.N. Singh, J.-F. Koenig, G. Poillerat and P. Chartier, *J. Electrochem. Soc., 137* (1990) 1408.